Mon. Not. R. Astron. Soc. **000**, 000–000 (0000) Printed 30 September 2008 (MN LATEX style file v2.2)

The Mid-Infrared [S IV]/[Ne II] versus [Ne III]/[Ne II] Correlation

Brent Groves⋆, Bas Nefs, & Bernhard Brandl
Sterrewacht Leiden, Leiden University, Niels Bohrweg 2, NL-2333 CA Leiden, The Netherlands

arXiv:0810.0010v1 [astro-ph] 30 Sep 2008

Received ¡date¿ / Accepted ¡date¿

ABSTRACT
The mid-infrared ratio [Ne III]$_{15.6\mu m}$/[Ne II]$_{12.8\mu m}$ is a strong diagnostic of the ionization state of emission line objects, due to its use of only strong neon emission lines only weakly affected by extinction. However this ratio is not available to ground-based telescopes as only a few spectroscopic windows are available in the MIR. To deal with this problem we aimed to verify if there exists a conversion law between ground-accessible, strong MIR line ratio [S IV]/[Ne II] and the diagnostic [Ne III]/[Ne II] ratio that can serve as a reference for future ground-based observations. We collated the [S IV]$_{10.5\mu m}$, [Ne II]$_{12.8\mu m}$, [Ne III]$_{15.6\mu m}$ and [S III]$_{18.7\mu m}$ emission line fluxes from a wide range of sources in the rich *Spitzer* and ISO archives, and compared the [Ne III]/[Ne II], [S IV]/[S III], and [S IV]/[Ne II] ratios. We find a strong correlation between the [S IV]/[Ne II] and [Ne III]/[Ne II] ratio, with a linear fit of log([Ne III]/[Ne II]) = 0.81 log([S IV]/[Ne II]) +0.36, accurate to a factor of ∼2 over four orders of magnitude in the line ratios. This demonstrates clearly the ability of ground-based infrared spectrographs to do ionization studies of nebulae.

Key words: Infrared:ISM–H II Regions–Planetary Nebulae–Galaxies:starburst

1 INTRODUCTION

The mid-infrared spectrum (MIR, ∼3-40μm) hosts a range of important diagnostic fine-structure emission lines. Due to the much lower dust opacity at these long wavelengths, the emission lines are significantly less affected by extinction than ultraviolet or optical lines (see e.g. Draine 2003). Thus these lines are able to probe ionized regions that lie behind dense obscuring clouds or even deep within galaxy centers, giving insights into the regions where massive star formation events actually occur, or heavily obscured active galactic nuclei (AGN) can exist.

One of the more useful facets of this wavelength regime is that it includes emission lines from several ions of the same species, in particular strong lines from neon and sulphur. These lines can be used as strong diagnostics of the ionization state of the emitting gas as, being from the same species, there is no direct dependence on the gas phase abundances, and the different ionization potentials allow the observer to trace the hardness of the ionizing spectrum (see e.g. Dopita & Sutherland 2003). Lines ratios such as [Ne V]$_{14.3\mu m}$/[Ne II]$_{12.8\mu m}$, [Ne III]$_{15.6\mu m}$/[Ne II]$_{12.8\mu m}$, and [S IV]$_{10.5\mu m}$/[S III]$_{18.7\mu m}$ have been used to diagnose the presence of deeply buried AGN (e.g. Sturm et al. 2002; Armus et al. 2006) and as indicators of the ages of starbursts (e.g. Achtermann & Lacy 1995; Thornley et al. 2000).

The major drawback of the MIR emission lines as diagnostics is their accessibility, with the full range of lines only available to spectrographs aboard space-borne telescopes like the *short wavelength spectrograph* (SWS, de Graauw et al. 1996) aboard the *Infrared Space Observatory* (ISO, Kessler et al. 1996) and the *infrared spectrograph* (IRS, Houck et al. 2004) aboard the *Spitzer Space Telescope* (Werner et al. 2004). While MIR instruments on ground based telescopes can provide higher spatial and spectral resolution, only a sparse number of MIR bands are available due to the opaqueness of the Earth's atmosphere in the mid-infrared (M-band:∼ 4.5 - 5μm, N-band:∼ 8.5 - 13μm, and Q-band:∼ 17 - 23μm). As a result, the [Ne III]$_{15.6\mu m}$ line is inaccessible from the ground and therefore recent high-resolution studies have resorted to the ratio [S IV]$_{10.5\mu m}$/[Ne II]$_{12.8\mu m}$ as a diagnostic (e.g. Snijders et al. 2007), in a similar manner to earlier aircraft-borne IR telescope studies (e.g. Achtermann & Lacy 1995). However the question remains whether the use of this ratio as a proxy for the ionization sensitive [Ne III]$_{15.6\mu m}$/[Ne II]$_{12.8\mu m}$ ratio is justified. While photoionization theory clearly indicates that there will be a correlation between these ratios, the dependence of the line emission on often unknown physical parameters make the accuracy of this correlation uncertain. As an example, the [S IV]/[Ne II] ratio is directly proportional to the sulfur to neon abundance ratio, while the [Ne III]/[Ne II] will be almost unaffected by any changes in the relative abundances. Similarly, with an excitation potential of 34.79 eV, [S III] is sensitive to lower energy photons than [Ne III], which has an excitation potential of 40.96eV and will not exist in photoionized gas when there are no photons above this limit.

In this letter we use archival ISO and *Spitzer* observations of a range of astrophysical objects to demonstrate that such a correlation does exist and derive a simple conversion law for these ratios. We mention possible systematics with the determination of these ratios and discuss the origin of the observed correlation. As a final note

⋆ brent@strw.leidenuniv.nl

Table 1. Publications from which we sourced our MIR emission lines differentiated the object classes, along with the telescope used and the mean fractional error in the [Ne II]$_{12.8\mu m}$ line.

Objects	σ_{NeII}/[Ne II]	Publication
Galactic H II regions	0.30	Giveon et al. (2002)[2]
Giant H II regions	0.15	Lebouteiller et al. (2008)[1]
Extragalactic		
H II regions & nuclei	0.05	Dale et al. (2006)[1]
M101 H II regions	0.39	Gordon et al. (2008)[1]
M83 H II regions	0.01	Rubin et al. (2007)[1]
M33 H II regions	0.01	Rubin et al. (2008)[1]
M82 Pointings	0.15	Beirão et al. (2008)[1]
Arp244 Pointings	0.04	Brandl et al. (2008)[1]
Starburst galaxies	0.09	Brandl et al. (2006)*[,1]
Starburst galaxies	0.30	Verma et al. (2003)[2]
BCDs	0.04	Wu et al. (2008)[1]
BCDs & Starbursts	0.09	Engelbracht et al. (2008)[1]
ULIRGs	0.10	Farrah et al. (2007)[1]
AGN	0.42	Sturm et al. (2002)[2]
AGN	0.14	Deo et al. (2007)[1]
LMC & SMC PNe	0.11	Bernard-Salas et al. (2008)[1]

1 : *Spitzer*
2 : *ISO-SWS* ∗ : Private Communication

we recommend the application of these results in future (ground-based) observations.

2 OBSERVATIONAL DATA

The strong, diagnostic, MIR emission lines [S IV]$_{10.5\mu m}$, [Ne II]$_{12.8\mu m}$, [Ne III]$_{15.6\mu m}$, and [S III]$_{18.7\mu m}$ have been detected and characterised in a broad range of astrophysical objects, from nearby galactic H II regions to ultraluminous infrared galaxies (ULIRGs). To determine the connection between the [S IV]/[Ne II] and [Ne III]/[Ne II] ratios we have extracted from the recent literature the fluxes of these four emission lines. While not exhaustive, the sample of 355 emission line objects is representative of the range of sources from which these lines arise, covering a range of physical parameters, such as source morphology and geometry, nature of the ionizing sources and metal and dust abundances.

A list of the different source types in our sample and the relevant papers from which we extracted these is given in Table 1. Included in the sample are sources ionized by massive stars, both small scale (H II regions and extragalactic H II regions) and large scale (blue compact dwarfs (BCDs), starburst galaxies (SB), and Ultra Luminous IR galaxies (ULIRGs)), planetary nebulae (PNe), which are ionized by white dwarfs, and active galactic nuclei (AGN).

The table also includes the average percentage uncertainty in the [Ne II] line as given in the reference. This uncertainty varies greatly between the various references, as the different authors have used different methods to account for both the observational and systematic uncertainties for their sources, which vary in flux and exposure times. While these uncertainties may bias our fit, the close correlation observed and the varying sizes of the samples (both discussed in the next section) will tend to minimize these effects. The given line uncertainties in the references were carried over when calculating their corresponding ratios.

The majority of objects within our sample were observed with the *Spitzer* IRS, with the remainder coming from ISO SWS observations (as noted in Table 1). In the cases where objects were observed twice (for example with both *Spitzer* and ISO), we have included both observations, to indicate the systematic uncertainty in the sample. For all of our sample, all four MIR lines fall within *Spitzer*'s IRS short-high (SH) module (9.9-19.6μm) and ISO's SWS (2.38 to 45.2μm), meaning that aperture effects are limited to that due to the different wavelengths of the lines in the ratios (a factor of 1.2 for [S IV] to [Ne II] and [Ne II] to [Ne III]).

Within our total sample there are approximately 8 objects observed by both telescopes, and a similar number of objects observed by *Spitzer* whose lines have been extracted by two different authors using different methods. For objects by both telescopes (e.g. NGC 4151), the difference in line ratios is of the order of 0.3 dex, most likely due to the different telescope apertures and pointings. Some objects were observed once by ISO, but have multiple pointings by *Spitzer*-IRS (e.g. M82), and for these objects we consider the ISO observation an integrated flux and the IRS observations to be individual H II regions. For the few IRS observed objects investigated by different authors, the differences in line ratios arise purely due to the different line flux extraction techniques (e.g. IIZw40) and are of the order of 0.2 dex, and within the given uncertainties. However the small number of objects observed multiply (~15, distributed across both AGN and Starburst/BCD) compared to the total sample size (355), mean that a bias of the final fit towards these types of objects will not occur.

In extracting our sample we excluded all objects in which any of the four lines were undetected, or for which only upper limits were provided. This means that we do have a bias in the sample against weak line objects, but, with objects covering a broad range of distances and four orders of magnitude in line ratio, this bias is likely to be weak. This bias is present, however, in at least one of the groups (ULIRGs), and is discussed further in the next section.

The total sample represents a large variety in ionising conditions ($-2.1 <$log([Ne III]/[Ne II])< 1.8), metal abundances (ranging from log(O/H) + 12 $\approx$ 7.1 (SBS 0335–052W) to $\approx$ 8.8 (IC342)) and the object particulars such as infrared luminosities (PNe to ULIRGs), galaxy types (blue compact dwarf galaxies to massive ULIRGs), and star formation rates (BCDs and H II regions of less than a few $M_\odot$ yr^{-1} to ULIRGs ~ 100's $M_\odot$ yr^{-1}).

3 RESULTS & DISCUSSION

The final sample of 355 emission-line objects is presented in figure 1 in the form of two emission line diagnostic diagrams: [S IV]/[S III] vs [Ne III]/[Ne II] (figure 1a) and [S IV]/[Ne II] vs [Ne III]/[Ne II] (figure 1b). The separate classes of object within the sample are differentiated both by colour and shape, as labelled in the key in the upper left hand corner of the diagrams. In the lower right corner of the diagrams we show the average observational uncertainty across the sample, as given within the references. As noted previously, the uncertainty given in the references varies significantly between the different classes, ranging from ~1% for M33 & M83 to ~40% for the galactic H II regions. In all classes however, the uncertainty on the [Ne III]/[Ne II] ratio is lower than that of the other two ratios considered here, partly due to the strength of the neon lines (higher signal-to-noise), but mostly due to the location of the [S IV]$_{10.5\mu m}$ in the silicate absorption feature (discussed further below), which both decreases the strength of this line and adds an additional uncertainty due to extinction. In any case, these uncertainties are applied to the reduced χ^2 fit discussed below.

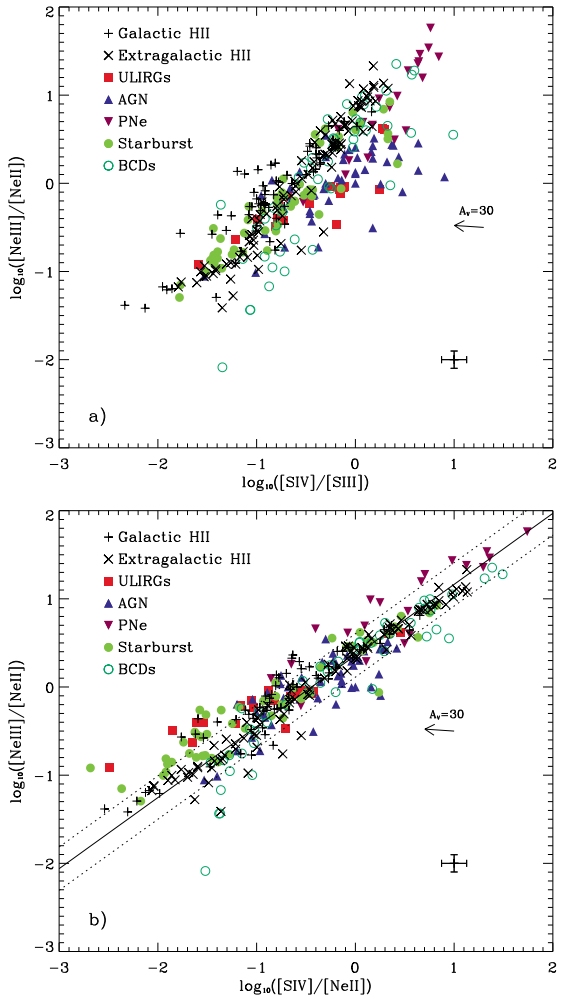

Figure 1. Mid-IR line ratio diagrams revealing the correlation between $[Ne\,III]_{15.6\mu m}/[Ne\,II]_{12.8\mu m}$ and $[S\,IV]_{10.5\mu m}/[S\,III]_{18.7\mu m}$ (a), and $[Ne\,III]_{15.6\mu m}/[Ne\,II]_{12.8\mu m}$ and $[S\,IV]_{10.5\mu m}/[Ne\,II]_{12.8\mu m}$ (b). Each diagram contains the observed ratios from several different emission-line objects, differentiated by colour and shape, as labelled by the key in the upper left hand corner, and discussed in section 2. The error bars in the lower right of the diagrams indicate the average uncertainty for the whole sample. The arrow indicates the effect of extinction on the ratios for an $A_V = 30$ magnitudes. The lower diagram also shows our best fit to the ratios (solid line) along with the 1-σ dispersion (dotted lines), as given in Table 2.

In both diagrams we plot a vector that indicates the effects of an $A_V = 30$ magnitudes of extinction on the line ratios by a uniform dust screen, assuming a Li & Draine (2001) extinction curve. Note that, depending on which curve is assumed, the length and direction of the extinction vector can change but that in all cases, the $[S\,IV]_{10.5\mu m}$ line suffers the highest relative extinction (see Table 2 and associated discussion in Farrah et al. 2007).

The first diagram, figure 1a, reveals the standard space-based diagnostic for the average ionization state of the emission line object. This diagram is a strong diagnostic as it uses 4 strong lines, with each ratio involving two different ionization states of the same element, meaning that abundance differences are not an issue. Due to this ionization dependence and insensitivity to abundance, this diagram has been often used in the literature as a measure of the average hardness of the ionizing radiation field, most recently by Gordon et al. (2008). In Gordon et al. (2008), the correlation between the [S IV]/[S III] and [Ne III]/[Ne II], clearly visible in our figure 1a, was quantified for both individual H II regions in M101 and for a combined M101 and starburst/BCD galaxy sample from Engelbracht et al. (2008) (their equations 5 and 6 respectively). They find a steeper slope than appears in figure 1a (1.53 versus 1.29), but this may be due to the smaller sample size, and is also biased by the Engelbracht et al. (2008) starburst sample. This sample, marked as BCDs in our sample, can be seen as the offset empty circles at low [Ne III]/[Ne II] in figure 1a. The visible offset from the rest of the sample may be intrinsic, but may also be from the underestimation of the contribution from the 12.7μm PAH feature in these weaker line objects (Smith et al. 2007).

Table 2. Fit parameters for the full sample and individual classes, including the number of objects (N) within the sample.

Object class	N	α	β	$\sigma_{Y\|X}$
Full sample	355	0.81	0.36	0.25
H II regions	65	0.74	0.42	0.23
Extragalactic H II	97	0.82	0.36	0.15
ULIRGs	20	0.49	0.26	0.33
AGN	20	0.69	0.29	0.25
PNe	20	0.74	0.56	0.30
Starburst	56	0.65	0.32	0.28
BCDs	49	0.86	0.32	0.30

There are several offset groups within figure 1a, the most noticeable being the AGN. This group is clearly offset towards higher [S IV]/[S III] values relative to their [Ne III]/[Ne II] ratio. The reason for this offset is uncertain, but is most likely related to the harder, power-law ionizing spectrum found in AGN. This leads to higher average electron temperatures in the S^{++} and Ne^{+} zones and different extents, relative to gas ionized by stars, and therefore a weaker [S III]/[Ne II] ratio for AGN relative to stellar photoionization. This offset may also be measurement related, with the weaker 12.7μm PAH feature meaning that the [Ne II] line is determined more accurately and with higher flux. The presence of ULIRGs and some starburst galaxies in this region as well is unsurprising as some of these sources contain known active nuclei, just as many of the AGN classified galaxies also have strong, active star formation.

In figure 1b we show the ground-accessible ratio [S IV]/[Ne II] versus [Ne III]/[Ne II], revealing a strong correlation between the ratios, justifying the use of the [S IV]/[Ne II] ratio as a surrogate for the [Ne III]/[Ne II] ratio when unavailable. Compared with figure 1a, the data show surprisingly less scatter. This probably arises due to the use of a common denominator ([Ne II]), but the [S III] line may also be introducing some scatter into figure 1a, possibly due to its longer wavelength (and hence lower resolution).

To quantify this correlation we perform a linear least-squares fit to the full sample using the IDL routine FITEXY, giving the empirical relationship,

$$\log([NeIII]/[NeII]) = \alpha \log([SIV]/[NeII]) + \beta. \quad (1)$$

The result of this fit, along with the 1 σ dispersion, is given in Table 2.

The first thing to note is that the log-space linear fit to the full sample appears to be accurate to 0.25 dex (that is, less than a factor of ~2 in the linear ratio) over four orders of magnitude in the line ratios, demonstrating clearly the ability of ground-based IR spectrographs to do ionization studies of nebulae. The dispersion around this relation is greater than the average uncertainty, indi-

cating either inaccurate uncertainties, intrinsic variations due to the variety of sources or, most likely, a combination of both.

In addition to the full fit we also present fits to our various object classes, also presented in Table 2. Overall, the relations match reasonably well with the full sample fit, with the two major outliers either side being the planetary nebulae (high offset in β) and the ULIRGs (shallow slope in α). These individual fits can be used when the specific class of objects being observed are known, but we suggest that the full fit should be used in most circumstances, as it is a more robust fit and includes all object classes.

In figure 1b the PNe are visibly offset from the rest of the sample, both to high [S IV]/[Ne II] and higher than average [Ne III]/[Ne II]. This offset is most likely due to the hotter and harder white dwarf ionizing source in PNe, although this then poses the question why the AGN, which also have a harder ionizing spectrum than that found in H II regions and galaxies, is not also more offset.

The shallow slope of the ULIRG sample demonstrates one of the issues with the [S IV]/[Ne II] ratio: the location of the $[\mathrm{S\,IV}]_{10.5\mu\mathrm{m}}$ in the 9.7μm silicate absorption feature. Of the Farrah et al. (2007) sample of 53 ULIRGs over half have no detections or upper limits for the [S IV] line, while a large fraction of those which do have detections are uncertain, with detections of less than 3 sigma. As noted in the paper, only in ULIRGs with low silicate depths ($S_{\mathrm{sil}} \lesssim 2.1$) is the [S IV] feature detected, even when the $[\mathrm{Ne\,III}]_{15.6\mu\mathrm{m}}$ line is present. Thus there is likely both a bias in our ULIRG sample and an offset, such that low [S IV]/[Ne II] ULIRGs are also those with high extinction and therefore offset from the relation, while the highest extinction sources are not included at all..

Another spectral feature which may affect the line ratio relation is the 12.7μm PAH feature seen clearly in many galaxy spectra (Smith et al. 2007). This broad feature lies below the [Ne II] line, and makes the determination and subtraction of the underlying continuum difficult, and thus increases the uncertainty in the flux of this line. As mentioned before, this may explain the offset seen in the Engelbracht et al. (2008) sample.

However, even with these outliers the correlation is surprisingly tight. Simple photoionization theory expects such a correlation, with higher ionization leading to higher values for both ratios (Dopita & Sutherland 2003), but variations in the ionization parameter[1] and ionizing spectrum cause different changes in the two ratios. Such variations have been explored in the case of starbursts and H II regions in Thornley et al. (2000) and Rubin et al. (2008) and, given these results, the tight fit indicates a close correlation between ionization parameter and spectral hardness in these objects.

One further issue is abundance variations. The [Ne III]/[Ne II] ratio is sensitive to abundance variations only indirectly, through the resulting temperature effects. The [S IV]/[Ne II] ratio however, can be directly affected by variations between the sulphur and neon abundances. As both are primary elements, significant total abundance variations are not expected. However, depletion of sulphur onto dust may cause variations in the gas phase and hence in the emission lines. While the total depletion of sulphur onto dust is uncertain (though see Lebouteiller et al. 2008), it does not seem to be a great effect on the Ne/S ratio, as shown by Rubin et al. (2007, 2008), and therefore on the [S IV]/[Ne II] ratio.

Thus, in summary, to determine whether it is reasonable to use the ground-accessible ratio $[\mathrm{S\,IV}]_{10.5\mu\mathrm{m}}/[\mathrm{Ne\,II}]_{12.8\mu\mathrm{m}}$ as a replacement for the diagnostic [Ne III]/[Ne II] ratio, we have collated existing ISO and *Spitzer* spectral observations of a wide range of astrophysical objects from the literature. We find a good correlation between these ratios with a linear fit giving the relation,

$$\log([\mathrm{NeIII}]/[\mathrm{NeII}]) = 0.81 \log([\mathrm{SIV}]/[\mathrm{NeII}]) + 0.36,$$

with a 1 σ dispersion of 0.25, corresponding to an uncertainty in the estimated line ratio of $\sim$ 70%. We propose that for future ground based observations this relationship be used to determine the ionization state of the observed objects, though note that caution must be applied when looking at heavily extinguished ($A_{\mathrm{V}} \gtrsim 20$) objects where the $[\mathrm{S\,IV}]_{10.5\mu\mathrm{m}}$ may be affected by the 9.7μm silicate absorption feature.

[1] The ionization parameter is a measure of the ionizing photon density over the gas density; $U = Q_{\mathrm{tot}}/n_{\mathrm{H}}c$, where $Q_{\mathrm{tot}} = \int_{13.6\mathrm{eV}} F_\nu/h\nu \, d\nu$

ACKNOWLEDGMENTS

Part of this work was supported by the German *Deutsche Forschungsgemeinschaft, DFG* project number Ts 17/2–1.

REFERENCES

Achtermann, J. M., & Lacy, J. H. 1995, ApJ, 439, 163
Armus, L., et al. 2006, ApJ, 640, 204
Beirão, P., et al. 2008, ApJ, 676, 304
Bernard-Salas, J., Pottasch, S. R., Gutenkunst, S., Morris, P. W., & Houck, J. R. 2008, ApJ, 672, 274
Brandl, B. R., et al. 2006, ApJ, 653, 1129
Brandl, B. R., et al. 2008, ApJ, submitted
Dale, D. A., et al. 2006, ApJ, 646, 161
Deo, R. P., Crenshaw, D. M., Kraemer, S. B., Dietrich, M., Elitzur, M., Teplitz, H., & Turner, T. J. 2007, ApJ, 671, 124
Dopita, M. A., & Sutherland, R. S. 2003, Astrophysics of the diffuse universe, Berlin, New York: Springer, 2003. Astronomy and astrophysics library, ISBN 3540433627
Draine, B. T. 2003, ARA&A, 41, 241
Engelbracht, C. W., Rieke, G. H., Gordon, K. D., Smith, J.-D. T., Werner, M. W., Moustakas, J., Willmer, C. N. A., & Vanzi, L. 2008, ApJ, 678, 804
Farrah, D., et al. 2007, ApJ, 667, 149
Giveon, U., Sternberg, A., Lutz, D., Feuchtgruber, H., & Pauldrach, A. W. A. 2002, ApJ, 566, 880
de Graauw, T., et al. 1996, A&A, 315, L49
Gordon, K. D., Engelbracht, C. W., Rieke, G. H., Misselt, K. A., Smith, J.-D. T., & Kennicutt, R. C., Jr. 2008, ApJ, 682, 336
Houck, J. R., et al. 2004, ApJS, 154, 18
Kessler, M. F., et al. 1996, A&A, 315, L27
Lebouteiller, V., Bernard-Salas, J., Brandl, B., Whelan, D. G., Wu, Y., Charmandaris, V., Devost, D., & Houck, J. R. 2008, ApJ, 680, 398
Li, A., & Draine, B. T. 2001, ApJ, 554, 778
Roche, P. F., & Aitken, D. K. 1984, MNRAS, 208, 481
Rubin, R. H., et al. 2007, MNRAS, 377, 1407
Rubin, R. H., et al. 2008, MNRAS, 387, 45
Smith, J. D. T., et al. 2007, ApJ, 656, 770
Snijders, L., Kewley, L. J., & van der Werf, P. P. 2007, ApJ, 669, 269
Sturm, E., Lutz, D., Verma, A., Netzer, H., Sternberg, A., Moorwood, A. F. M., Oliva, E., & Genzel, R. 2002, A&A, 393, 821

Thornley, M. D., Schreiber, N. M. F., Lutz, D., Genzel, R., Spoon, H. W. W., Kunze, D., & Sternberg, A. 2000, ApJ, 539, 641
Verma, A., Lutz, D., Sturm, E., Sternberg, A., Genzel, R., & Vacca, W. 2003, A&A, 403, 829
Werner, M. W., et al. 2004, ApJS, 154, 1
Wu, Y., Charmandaris, V., Houck, J. R., Bernard-Salas, J., Lebouteiller, V., Brandl, B. R., & Farrah, D. 2008, ApJ, 676, 970